

# The Behaviour of Pile Group and Combined Piled-Raft Foundation in Liquefiable Soil under Seismic Conditions

Aniruddha Bhaduri<sup>1</sup>, Vansittee Dilli Rao<sup>2</sup> and Deepankar Choudhury<sup>3</sup>

<sup>1,2</sup>Ph.D. Research Scholar, Department of Civil Engineering, Indian Institute of Technology Bombay, Mumbai 400076, India

<sup>3</sup>Institute Chair Professor, Department of Civil Engineering, Indian Institute of Technology Bombay, Mumbai 400076, India  
E-mail: dc@civil.iitb.ac.in

**ABSTRACT:** This paper highlights the beneficial usage of Combined Pile-Raft Foundation (CPRF) over conventional pile group foundation subjected to seismic loading in liquefiable soil. Firstly, a single pile resting on a liquefiable soil is numerically modelled and subsequently validated with available dynamic centrifuge test result by using finite difference based computer programme, FLAC3D. Thereafter, the model is extended for simulating CPRF and pile group. Further parametric studies are performed to understand the effect of pile spacing ( $s$ ), pile length ( $l$ ) and different seismic motions on the behaviour of CPRF and pile group. Results are presented in terms of normalised bending moment ( $M/M_{max}$ ), shear forces and pore water pressure (PWP) ratio. Increase in shear resistances in the range of (35 - 60)% and (40 - 70)% are observed for the piles in CPRF over the conventional pile group foundation, having a pile spacing of 2 to 5 times of its diameter ( $d$ ) and the ( $l/d$ ) of 14 to 20, respectively. These outcomes portray the advantages of employing CPRF over pile group founded in liquefiable area under seismic loading.

**KEYWORDS:** Liquefaction, CPRF, Pile Group, Centrifuge, FLAC3D

## 1. INTRODUCTION

Over the last few decades, CPRF has proven its merits as one of the most effective and economically feasible foundation system in the deep foundation segment. Burland et al. (1977) first discussed the rationality behind using pile below a raft foundation as settlement reducers. Since then, ample amount of research has been carried out in the field of CPRF, especially under static vertical loading, for apprehending the behaviour of this hybrid foundation system in a precise manner. Kumar & Choudhury (2018) proposed new prediction model for finding capacity of CPRF under static vertical loading considering different soil-structure interaction factors. Roy et al. (2018) incorporated the effect of superstructure on the behaviour of CPRF by using finite element method. International Society for Soil Mechanics and Geotechnical Engineering (ISSMGE) has published design guidelines for CPRF (Katzenbach & Choudhury 2013) under static loading condition. With the inception of modern high-speed computers, designing large CPRF systems became viable. Poulos & Davis (2005), Ibrahim et al. (2009) and Russo et al. (2013) detailed the fruitful use of CPRF beneath the high rises like Emirates Twin Towers, Pentominium Tower and Burj Khalifa in Dubai, respectively. Kumar et al. (2015, 2016, 2017a,b), Kumar & Choudhury (2017) used various numerical simulation techniques in assessing the behaviour of CPRF for several structures. Poulos (2001) corroborated the credibility of combined pile-raft foundation as the most desired foundation solution when displacement based framework is adopted. Approximate numerical solution for analysing piled-raft foundation has also been proposed (Poulos 1994). Viggiani (2001), Poulos et al. (2011), Poulos (2016, 2017) abbreviated a number of case studies of foundation solutions used for tall buildings and furnished generalised design solutions for the same, in a methodical manner. Reul and Randolph (2004) studies CPRF subjected to non uniform vertical loads. Katzenbach et al. (2016) had abstracted several case studies in Germany where CPRF has been used.

Apart from static loading, experimental and numerical research has been performed to interpret the behaviour of CPRF under dynamic loading. Horikoshi et al. (2003a) and Matsumoto et al. (2004) performed a series of shaking table tests on piled-raft foundation situated on sand by using the geotechnical centrifuge. Ghosh & Madabhushi (2007) performed a number of dynamic centrifuge modelling as a tool to investigate the foundation response of a typical power plant like structures founded on layered soil deposit. Dash et al. (2009) performed a case study on the Kandla port and Customs office Tower located in Kandla Port, India which was

hit by the 2001 Bhuj earthquake. Post-earthquake investigation revealed the chance of liquefaction of the sand layer below clay. Phanikant et al. (2013), Choudhury et al. (2015), Chatterjee et al. (2015, 2019) studied the behaviour of pile in liquefiable soil. Yamashita et al. (2012) monitored the static and seismic behaviour of a piled-raft foundation of a base isolated building in Tokyo, founded in a layered soil deposit, from the beginning of the construction to 43 months after the end of the construction. Kumar & Choudhury (2016) executed the static and seismic analysis of pile foundation for an oil tank in Iraq.

Although plenty of work has been carried out to grasp the behaviour of CPRF under various loading, immense scope lies ahead in the dynamic front. In a non-homogeneous soil condition, where the intermediate soil layer is prone to liquefaction, pile foundations are used conventionally. Implementing CPRF in a liquefiable zone is still not the preferred choice of the designers, whereas in a displacement based framework, a number of advantages may give CPRF the edge over pile foundations. This paper presents a comparative study between CPRF and traditional deep foundation under various seismic loading conditions. First a single pile is numerically modelled in finite difference based computer program FLAC3D, v4.0 (ICG 2009) and successively validated with available dynamic centrifuge test results. Thereafter, the numerical model is extended for modelling pile group and CPRF under similar soil conditions. Parametric studies are performed to investigate the effects of pile spacing ( $s$ ), pile length ( $l$ ) and various real earthquake loadings on pile group and CPRF, in a comparative approach. Results are presented in terms of normalised bending moment ( $M/M_{max}$ ), shear forces along the pile lengths and pore water pressure (PWP) ratio. The present study is helpful in adopting the foundation type to be used in a liquefaction prone area.

## 2. NUMERICAL MODELLING AND VALIDATION

### 2.1 Numerical Simulation of Single Pile

Figure 1 depicts the numerical model of the single pile founded in the layered soil. The soil has a three layered profile, where the liquefiable Nevada sand layer is sandwiched between the Slightly Cemented Sand layer on top and bottom. The top and bottom layers possess a thickness of 2m each, and the liquefiable Nevada sand layer is having a thickness of 6m and the water table is assumed to be situated at the top of the soil. The pile is having a length of 10m with a diameter of 0.6m as reported by Abdoun et al. (2003). Pile is modelled as the pile element embedded in the standard library of FLAC3D, whereas while

modelling the raft or pile cap for the parametric studies, linearly elastic isotropic material constitutive model is used.

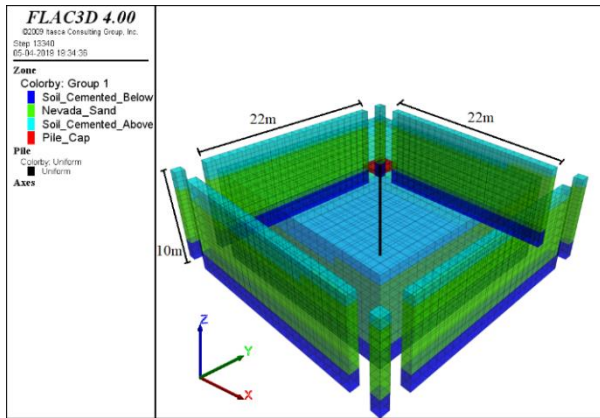


Figure 1 Single pile in layered soil with free field boundary

Mohr-Coulomb elastic perfectly plastic constitutive model is used for modelling the soil layers for static loading. For the static gravity analysis, the bottom boundary of the model is restrained from moving in all the directions and the side boundaries of the model are assumed to be as roller boundaries which refute any horizontal movement and permits only vertical movement. The properties of the soil layer along with the pile are given in Table 1.

Table 1 Material Properties (after Abdoun et al. 2003, Chatterjee & Choudhury 2018 and Chatterjee et al. 2019)

Property	Type of Soil		Pile
	Nevada Sand Layer	Slightly Cemented Sand Layer	
Young Modulus [ $E_s$ ], MPa	18	75	3200
Poisson Ration [ $\mu$ ]	0.31	0.40	0.36
Density [ $\rho$ ], kg/m <sup>3</sup>	1962	2038	2500
Relative Density [ $D_r$ ], %	40	---	---
Cohesion [ $c$ ], kPa	---	5.1	---
Friction angle [ $\phi$ ], °	30.0	34.5	---
Coefficient of Permeability [ $k$ ], m/s	$6.6 \times 10^{-5}$	$1.0 \times 10^{-10}$	---

For numerical simulation of liquefaction in the Nevada sand layer, Finn constitutive model is used which is inbuilt in the standard library of FLAC3D. This constitutive model incorporates the formulation proposed by Byrne (1991) into the standard Mohr-Coulomb model. The Byrne (1991) formulation sets the model parameters in terms of relative density of the soil layer. This formulation relates the increment of volume decrease ( $\Delta \epsilon_{vd}$ ) with the cyclic shear strain amplitude ( $\gamma$ ) as delineated in Eq. (1).

$$\frac{\Delta \epsilon_{vd}}{\gamma} = C_1 \exp\left(-C_2 \left(\frac{\epsilon_{vd}}{\gamma}\right)\right) \quad (1)$$

Here,  $C_1$  and  $C_2$  are constants.  $C_1$  can be directly formulated from relative density ( $D_r$ ), as given in Eq. (2), whereas  $C_2$  can be empirically correlated with  $C_1$  as depicted by Eq. (3).

$$C_1 = 7600(D_r)^{-2.5} \quad (2)$$

$$C_2 = \frac{0.4}{C_1} \quad (3)$$

For performing dynamic analysis, the corner and side boundaries are assumed to be free field boundaries. Here, the main grid of the model is attached with the free-field boundary with the aid of viscous dashpots which simulate a quite boundary condition. In this way, the free field grid provides identical situation of an infinite model boundary, where reflections of the upwardly propagating waves, back into the model are arrested, causing no undesirable distortion in the numerical simulation. Thus, free field boundary condition is required for dynamic analysis for absorbing waves reaching the boundary and hindering the reflection of the waves back into the numerical model.

Figure 2 denotes the ground motion applied at the base of the model as reported by Abdoun et al. (2003). The ground motion consists of 40 cycles of uniform acceleration comprising a prototype amplitude of 0.3g with a frequency of 2 Hz.

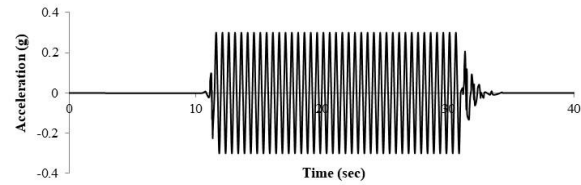


Figure 2 Input ground motion used for validation in present study

## 2.2 Validation of Numerical Model

Figure 3 denotes the comparison of the bending moment profile of the pile obtained from the numerical analysis with the same obtained from the centrifuge test results, at different time intervals of the motion.

Here, it can be noted that in the centrifuge model, the model is tilted by an amount of 2°. This type of configuration is made for modelling lateral spreading in the layered soil configuration. But in FLAC3D, due to numerical modelling constraint, it is not possible to model the 2° tilt at the base of the model as the ground motion can only be applied at a base which is horizontal. However, the top layers are modelled with the similar 2° tilt. Because of this numerical constraint, it can be deduced from Figure 3 that the moments at the top portion of the pile, perceived from the numerical model, are matching well with the experimental study, in comparison to the same at the bottom part of the model. Here, it is worth mentioning that due to less amount of lateral spreading in the bottom portion of the pile, stiffer soil prevails which generates larger moment. Thus, this comparison establishes the validity of the numerical model.

## 3. PARAMETRIC STUDY

For the purpose of parametric studies, a 2x2 CPRF model along with a similar 2x2 pile group model is chosen. Figure 4 represents the schematic representation of CPRF founded in the three layered soil profile. Here, the piles are having a length of 10m with a diameter of 0.5m. The square raft is having a thickness of 1m with a dimension of 4m. The raft configuration in the CPRF has been adopted as described by Horikoshi et al. (2003b). In this model, the cemented soil layer below the Nevada sand layer has been extended to greater depth of 10m. In all the cases, water table is assumed to be at the top of the soil model. All other dimensions of the soil box are same as shown in Figure 1.

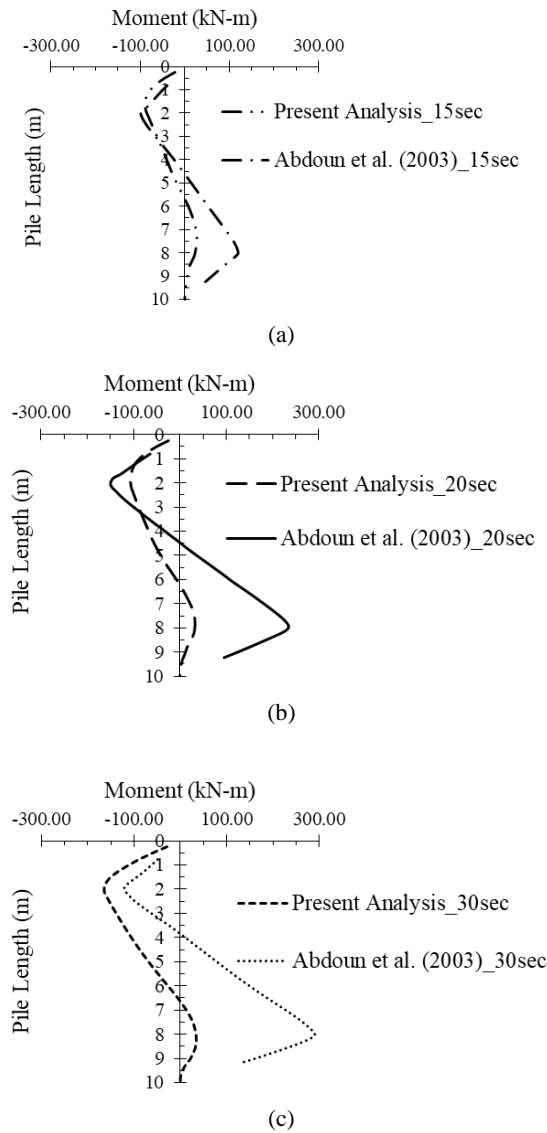


Figure 3 Comparison of bending moment profile with centrifuge test result after (a) 10sec (b) 20sec and (c) 30sec of the motion

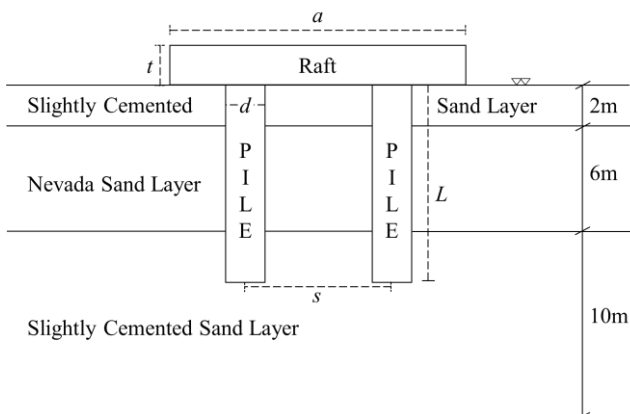


Figure 4 Schematic representation of CPRF for parametric study

All the motions for the parametric study are applied at the base of the model. Pile groups are modelled in a similar manner where the pile cap is elevated from the soil surface to deny the contact with it.

### 3.1 Effect of Pile Spacing

Pile spacing in both CPRF and pile group plays pivotal role in the behaviour of both types of foundations. Four different pile spacing to diameter ratios ( $s/d$ ) of 2, 3, 4 and 5 are considered for the analysis. The acceleration-time history as described in Figure 2 is applied at the base of all the models of CPRF and pile group for this analysis. Figure 5 delineates the comparison between the shear resistances of the front piles of CPRF with the same of the pile group. Here, an increase in the pile resistance of around 35% to 60% of the piles in CPRF over the pile group foundation can be observed for the front piles. For the rear piles, similar observations are made. Apart from the shear resistance of the piles, raft also shares considerable amount of load in CPRF. These outcomes ratiocinate that because of the presence of raft, the confining pressure beneath the CPRF system increases, which helps in mobilising more shear resistance in the piles of CPRF compared to the pile group. This phenomenon is attributable to the fact that in CPRF, raft shares considerable amount of load acting on the foundation system as the raft rests on the ground. Thus, part of the self-weight of the raft (along with superstructural load which acts on the system, if any) gets transferred to the soil via raft, which enhances the confinement beneath the raft. This phenomenon is missing for a conventional pile group foundation where the contact between the pile cap and soil is denied, which further refutes the self-weight of the pile cap to play any part in the behaviour of the foundation system.

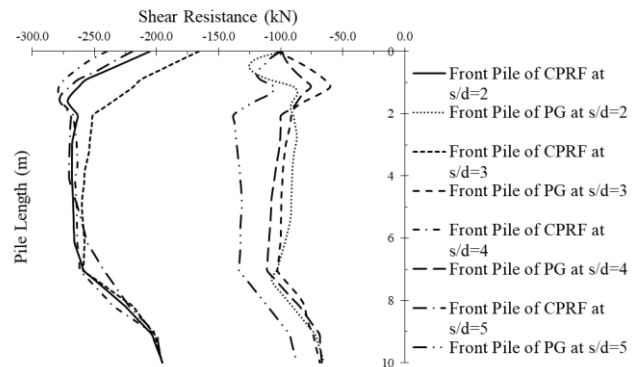


Figure 5 Shear resistance comparison between front piles of CPRF with the same with pile group at different  $s/d$

Figure 6 showcases the comparison between the moments of the front piles of CPRF with the same of pile groups. Here, it is to be noted that the piles in both CPRF and pile group undergo maximum bending moment at the top portion of it, whereas, along the liquefiable zone, the piles in CPRF experience a little lesser moment than that of pile group. Although for all  $s/d$  values, the piles in CPRF undergoes maximum bending moment at the top nodes, but for  $s/d$  of 3, the bending moment is considerably higher at the junction of the top cemented sand and liquefiable Nevada sand layer. This demonstrates the significance of strategic appointment of piles in earning maximum benefit of a CPRF system.

Figure 7 manifests the comparison between the PWP ratio of the CPRF system and the pile group for an  $s/d$  of 2. The location where the histories of PWP ratios were generated was at the middle of the liquefiable soil layer. From this demonstration, it can be clearly reckoned that with dynamic time, for CPRF the PWP ratio first increases, then becomes almost stable and at the end, exhibits an indication of decreasing trend. The maximum PWP ratio generated for CPRF is little below 0.8. On the contrary, for pile group, the PWP ratio keeps on increasing and reaches a maximum of around 0.84 at the end of the shaking. Similar observations can be made for  $s/d$  of 3, 4 and 5 as well. Also, while comparing the PWP ratio between CPRF having an  $s/d$  of 2 and 5, it is noticed that in the vicinity of the piles, PWP ratio for  $s/d$  of 2 is little less than the same for 5, which is justifiable as a smaller  $s/d$  value accounts for a more densely spaced piles which eventually increases the local densification.

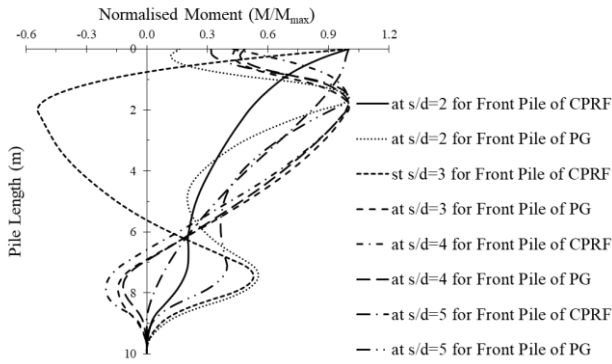
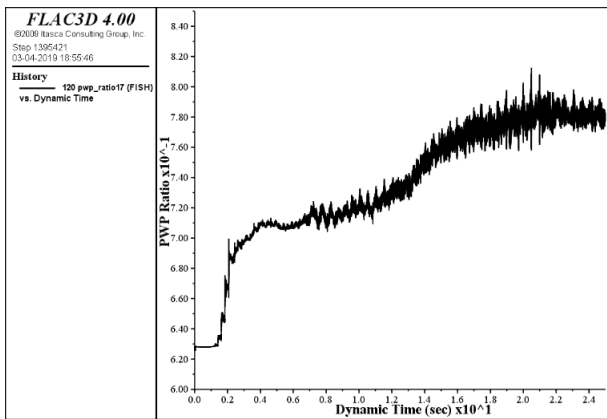
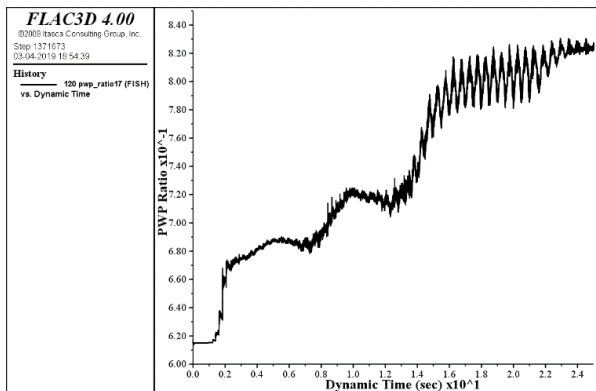


Figure 6 Moment comparison between front piles of CPRF with the same with pile group at different  $s/d$



(a)



(b)

Figure 7 PWP ratio at  $s/d$  of 2 for (a) CPRF and (b) Pile group at the middle of liquefiable layer

Abdoun et al. (2003) recognizes the fact that in similar circumstances, local densification occurs around the pile groups. When densification occurs near the piles, volume of the void ratio decreases which helps in expulsion of pore water from the vicinity of the piles to other parts of the soil model. In addition to the local densification provided by the piles, in CPRF, the raft rests on the soil, which again increases the confinement around the piles, more than a pile group. This phenomenon increases the effective stress which results in decreasing PWP ratio near the piles in the liquefiable layer. Thus it can be opined that, in the CPRF system, because of the raft, the confinement below the foundation system increases, which helps in decreasing the PWP ratio, while in the pile group, as the pile cap

does not rest on the ground surface, the only source of confinement comes from the piles.

### 3.2 Effect of Pile Length

Choosing the length of pile, especially when the foundation is situated in a liquefiable soil, is a major part in designing a deep foundation. Here, four different pile length ( $l$ ) to diameter ratio (i.e.  $l/d$  ratio), such as 14, 16, 18 and 20 are considered. The similar acceleration-time history as depicted in Figure 2 is applied at the base of all the models of CPRF and pile group for this analysis. Figure 8 demonstrates the comparison between the shear resistances of the front pile of CPRF with the same with pile group. Here it is noticed that an increase in shearing resistance of front piles of CPRF in the order of 40% to 70% occurs over the same of pile group under similar loading condition. Analogous conclusion can be drawn from the rear piles as well. This increase in shear resistance for the piles in CPRF can be attributable due to the increase in confinement provided by the raft. Also, from Figure 8, it can be perceived that for pile group having an  $l/d$  of 14 and 16 where the piles get terminated in the middle and end of the liquefiable zone, respectively, the maximum shearing resistance occurs at the top of it, while it drastically reduces when the piles enter the liquefiable Nevada sand layer. For higher  $l/d$  values of 18 and 20, as the bottom of the pile is embedded in the stiffer cemented sand layer, the shear resistances are observed to be more or less constant along the pile length. On the contrary, the shear resistance of the piles in CPRF maintains considerably higher resistance throughout its length. These behaviours highlight the utility of using CPRF in a liquefiable soil deposit.

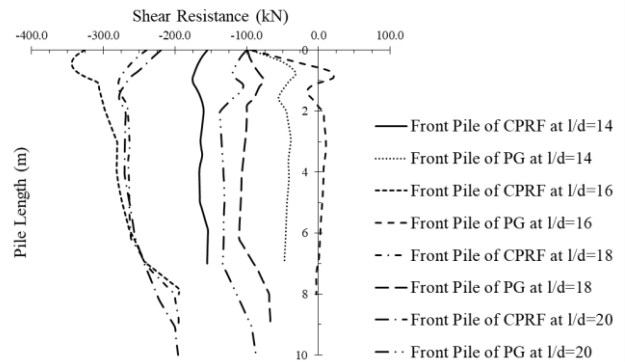


Figure 8 Shear resistance comparison between front piles of CPRF with the same with pile group at different  $l/d$

Figure 9 draws the comparison between the moments carried by the front piles of CPRF with the same of pile group. Here, in general, it can be clearly recognized that for both the cases, the maximum moment materializes at the top of the piles. It further reduces along the pile length and eventually converges to zero at the bottom of the pile. Further, a closer scrutiny on the bending moment diagram reveals that for  $l/d$  of 14 (i.e. a pile length of 7m), for CPRF, the maximum moment is generated at 2m below the surface which is nothing but the junction of the liquefiable and non-liquefiable layer, although at the very top node, the moment is considerably high. For similar pile length of pile group, the maximum moment occurs at the top node of pile. In this case, the piles are terminated in the liquefiable layer. For  $l/d$  of 16 (i.e. a pile length of 8m), the piles in CPRF generates maximum moment at the top pile node while for pile group, the maximum moment occurs at the junction of Nevada sand layer. Here, the piles are ended at the juncture of the Nevada sand layer and the cemented layer at the bottom. For  $l/d$  of 18 and 20 (i.e. a pile length of 9m and 10m, respectively), the maximum bending moment for the piles in both types of foundation occurs at the confluence of liquefiable and non-liquefiable layer, whereas at the top nodes, the moment is substantially lower. It can also be learnt that at the top

nodes, the piles of CPRF experiences much lesser bending moments compared to the pile group which can be attributable due to the effect of raft. Here, the pile bottoms are rooted in the cemented sand layer at the bottom.

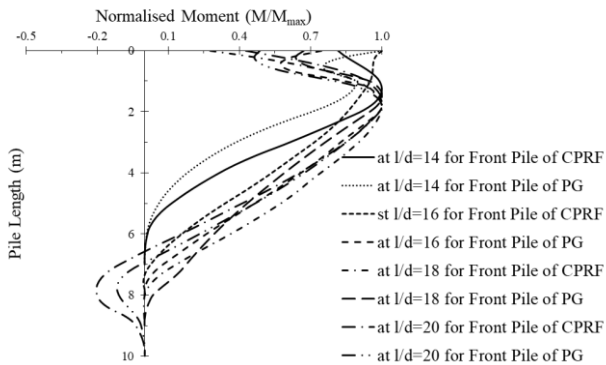


Figure 9 Moment comparison between front piles of CPRF with the same with pile group at different  $l/d$

Figure 10 portrays similar comparison between the rear piles of CPRF and pile group corresponding to the variation of pile length. Only difference can be spotted in the behaviour of rear pile of pile group having an  $l/d$  of 14, where unlike the previous case, the maximum bending moment occurs at the junction of the liquefiable layer.

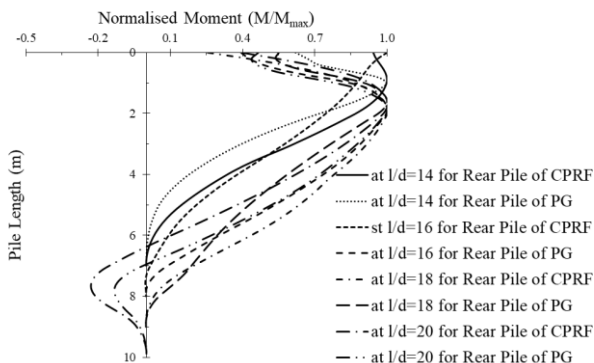


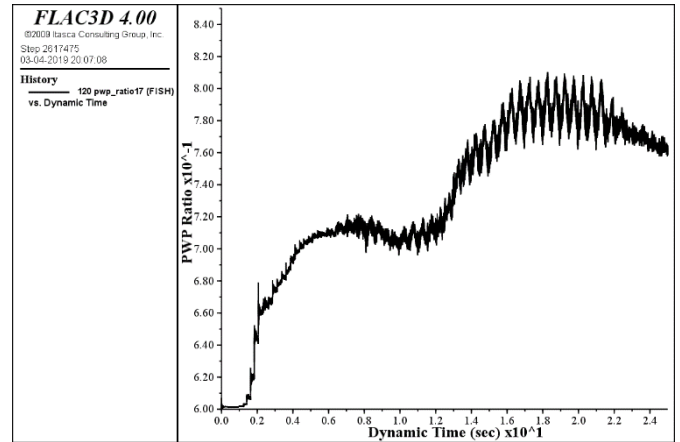
Figure 10 Moment comparison between rear piles of CPRF with the same with pile group at different  $l/d$

Figure 11 presents the comparison between the PWP ratio of the CPRF system and the pile group for an  $l/d$  of 14. The history of the PWP ratio throughout the dynamic time is captured at the bottom of the pile for both the cases. Here, it can be observed that for CPRF, at the initial stages of the dynamic time, the PWP ratio increases and after reaching an apex, reduces with time. On the contrary, for the pile group, the PWP ratio increases with time and after reaching a limit, becomes almost constant. This trend indicates the effect of increasing confinement due to raft in the CPRF system which is absent in the pile group.

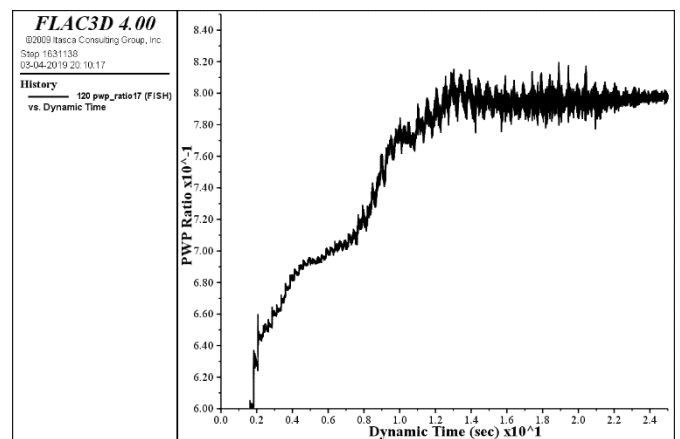
Figure 12 corresponds to the variation in PWP ratio for the foundation systems with an  $l/d$  of 18. Similar trend of PWP ratio can be seen in this case as well. For  $l/d$  of 18, the maximum PWP ratio experienced by the CPRF system at the bottom of the Nevada sand Layer is around 0.82 while it starts decreasing immediately before

becoming stable. For the pile group, the history of PWP ratio does not exhibit any trend of reduction and holds constant after reaching the apex.

From Figure 11(a) and 12(a) it can be further deduced that the PWP ratio is lesser for a higher pile length embedded in a more competent soil strata compare to the smaller pile length terminated in the liquefiable zone. These observations evince the importance of determining appropriate pile length and type of foundation to be adopted, especially in cases where piles are passing through a liquefaction prone area.



(a)

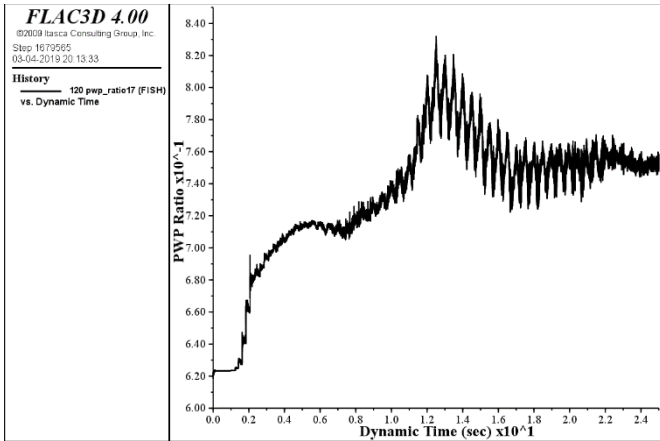


(b)

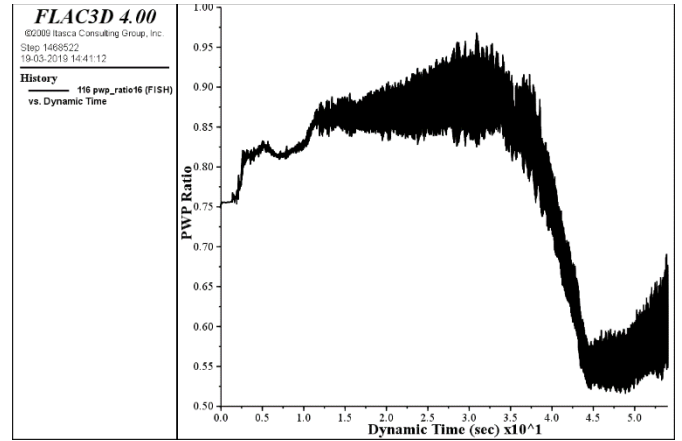
Figure 11 PWP ratio at  $l/d$  of 14 for (a) CPRF and (b) Pile group at the middle of liquefiable layer

### 3.3 Behaviour of CPRF and Pile Group under Different Ground Motions

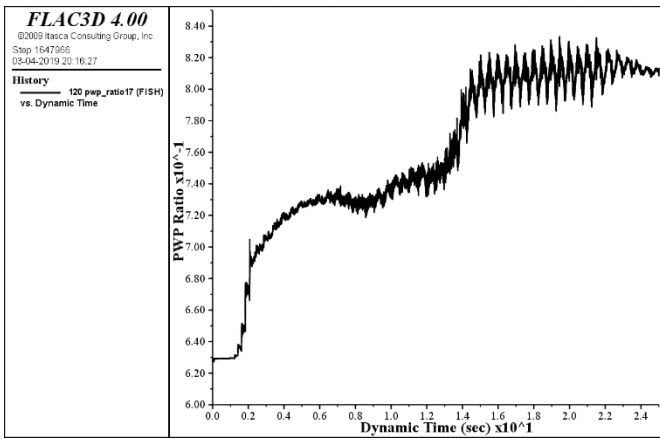
Investigating the behaviour of CPRF and pile group under real earthquake time-histories can be rendered as of utmost importance. For accomplishing the objective, two real acceleration time histories, which are of 1940 El-Centro, 1989 Loma-Prieta and 2011 Sikkim earthquakes, are incorporated in the model. The reason behind choosing these earthquake time histories is that these three set of ground motions represent a wider predominant frequency range of 2Hz to 5 Hz, a broad range of peak ground accelerations (PGA) from 0.201g to 0.331g, along with a dynamic time ranges from 40 seconds to 90 seconds. This provides a brief outlook on the behaviour of different foundations under a range of real seismic events.



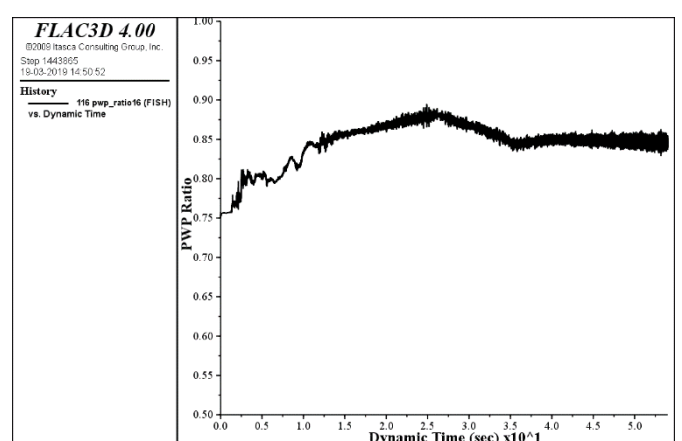
(a)



(a)



(b)



(b)

Figure 12 PWP ratio at  $l/d$  of 18 for (a) CPRF and (b) Pile group at the middle of liquefiable layer

Figure 14 PWP ratio for 1940 El-Centro earthquake for (a) CPRF and (b) Pile group at the middle of liquefiable layer

### 3.3.1 Effect of 1940 El-Centro Earthquake

Figure 13 depicts the acceleration time history of 1940 El-Centro earthquake.

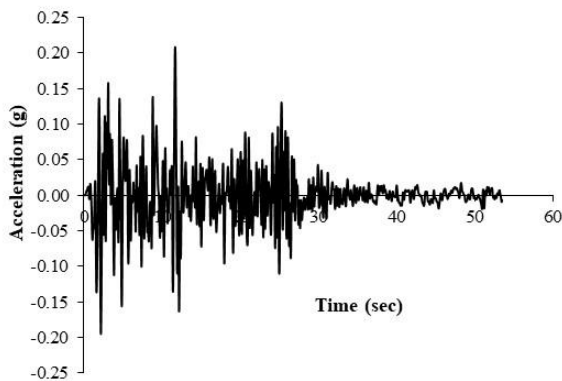


Figure 13 Input ground motion of 1940 El-Centro earthquake

The PGA of the earthquake is 0.201g whereas the magnitude is 6.9 with a predominant frequency of 2 Hz, having a dynamic time of 54 seconds. Figure 14 shows the comparison between the PWP ratio at the middle of the liquefiable layer near the piles of CPRF and pile group. From this comparison, it can be clearly concluded that due to the larger confining effect of CPRF, the PWP ratio decreases after reaching a peak. On the other hand, for pile group, it remains almost constant. Similar observations can be made in a location away from the piles, although the decreasing trend is less steep.

### 3.3.2 Effect of 1989 Loma-Prieta Earthquake

Figure 15 depicts the acceleration time history of 1989 Loma-Prieta earthquake.

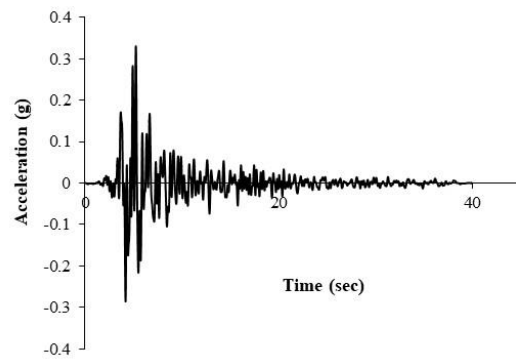
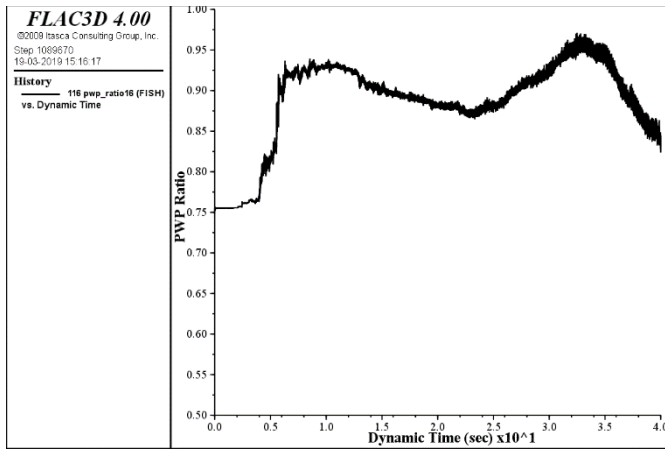
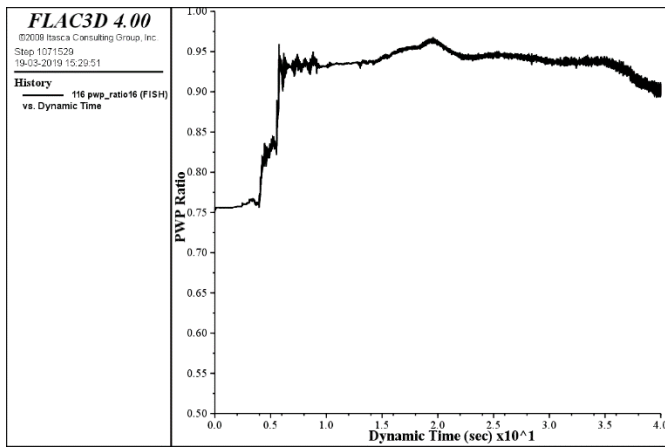


Figure 15 Input ground motion of 1989 Loma-Prieta earthquake

The PGA of the earthquake is 0.331g whereas the magnitude is 6.9 with a predominant frequency of 3.333 Hz, having a dynamic time of 40 seconds. Figure 16 shows the comparison between the PWP ratio at the middle of the liquefiable layer near the piles of CPRF and pile group. Comparative study elucidates that for CPRF, at the end of the ground shaking, the PWP ratio decreases while for pile group it remains constant. This again affirms the importance of raft on the overall performance of the foundation system. Similar trend is also observed in the far field, away from the foundation.



(a)



(b)

Figure 16 PWP ratio for 1989 Loma-Prieta earthquake for (a) CPRF and (b) Pile group at the middle of liquefiable layer

### 3.3.3 Effect of 2011 Sikkim Earthquake

Figure 17 delineates the acceleration time history of the 2011 Sikkim earthquake.

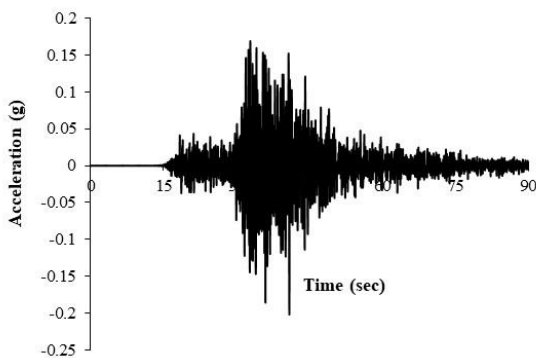
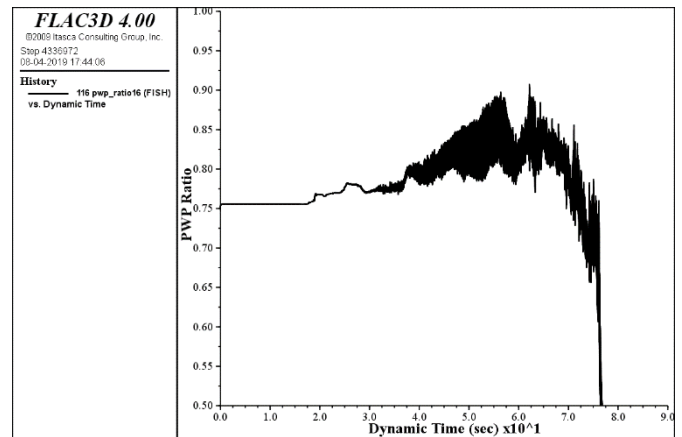


Figure 17 Input ground motion of 2011 Sikkim earthquake

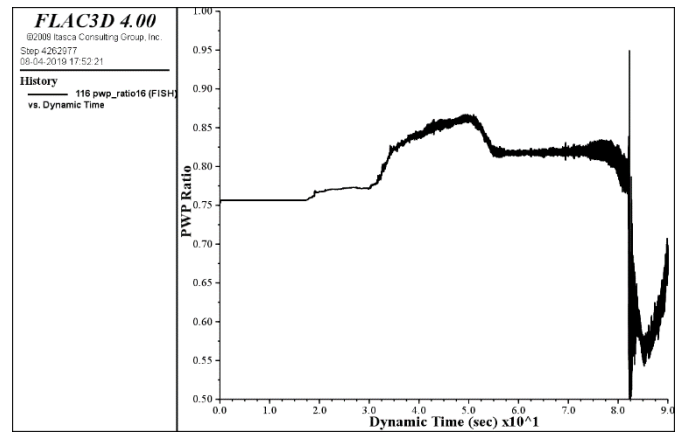
The PGA of the earthquake is 0.202g whereas the magnitude is 6.9 with a predominant frequency of 5 Hz, observed up to a dynamic time of 90 seconds. Figure 18 shows the comparison between the PWP ratio of CPRF and pile group near the foundation. Like the previous cases, here also the PWP ratio shows decreasing trend for CPRF whereas for pile group, erratic trends are observed.

These observations reaffirm the beneficial usage of CPRF over pile group foundations where PWP ratio is concerned in a liquefiable soil deposit. It is also worth noting that the advantageous inclusion of

raft can be favourable over a frequency range of 2 Hz to 5 Hz, with a dynamic time in the range of 40 seconds to 90 seconds, where seismic loading is acting.



(a)



(b)

Figure 18 PWP ratio for 2011 Sikkim earthquake for (a) CPRF and (b) Pile group at the middle of liquefiable layer

Besides these observations, it should be noted that in all these cases, the PWP ratio is observed at the middle of the liquefiable layer. At the top of the liquefiable layer, i.e. at the junction of Nevada sand layer and the slightly cemented top soil layer, in most of the cases the soil liquefies, irrespective of the type of foundations which are in use. This phenomenon may be attributable to the fact that because of the 2° tilt in the upper part of the soil, the susceptibility of liquefaction increases. Also, it should be noted that as the depth increases, effective stress increases accordingly, which eventually reduces the vulnerability of liquefaction. Apart from this, the ground motion applied at the base of the model gets amplified in the liquefied zone which causes the top layers subjected to liquefaction. These revelations help in comprehending the behaviour of deep foundations in a liquefiable zone, more coherently.

### 3.3.4 Comparison in Shear Resistance and Bending Moment

Figure 19 shows the comparison in shear resistances between the front piles of CPRF and the same of pile group. Here, it can be noted that the piles in CPRF contribute 50% to 80% more shear resistance than the piles in pile group. It is to be highlighted that for CPRF, the maximum shearing resistance occurs at the pile top and eventually decreases a little along the pile length. On the contrary, the piles in pile group maintain almost constant shearing resistance along the length of the pile. Figure 20 showcases the comparison in bending moment profile of rear piles in CPRF and that of pile group. Here for all the cases, the maximum bending moment occurs at the top of the

piles and further decreases and converges to zero at the bottom of it. The piles of CPRF experience lesser moment than those of pile group throughout the soil layers. The trends of the moment carrying capacity of front piles for both the foundation systems are also alike. These observations indicate the higher moment carrying capacity of pile in CPRF than their pile group counterpart.

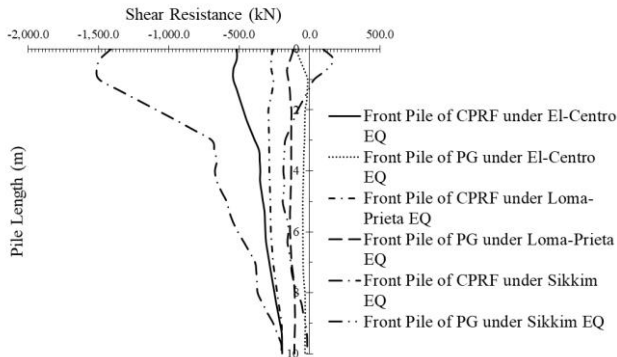


Figure 19 Comparison of shear resistance of piles in CPRF and pile group for different earthquakes

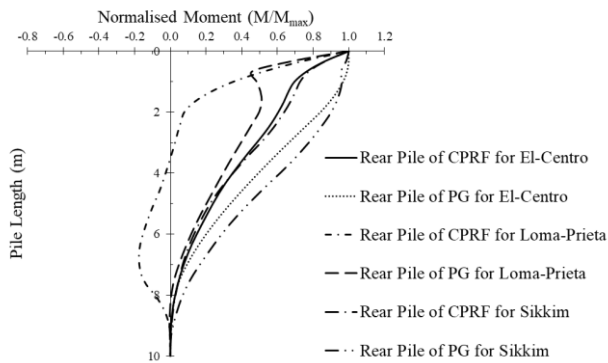


Figure 20 Comparison of moments of piles in CPRF and pile group for different earthquakes

#### 4. CONCLUSIONS

The present paper furnishes a comparative numerical study between the behaviour of CPRF and conventional pile group foundation situated in a liquefiable soil deposit, subjected to dynamic loading. Firstly the numerical model is validated with available dynamic centrifuge test result. Thereafter, the study is further extended to model CPRF and pile group founded in similar soil conditions, for performing parametric studies. For studying the effect of spacing, four different  $s/d$  ratios, namely 2, 3, 4 and 5 are considered. Here an increase in the shear resistance of piles in CPRF of 35% to 60% over the pile group is observed. This observation indicates the favourable effect of the inclusion of raft over conventional pile group foundation as raft improves the effective stress beneath the foundation. Also the piles of CPRF exhibit greater moment carrying capacity than that of pile groups. Although for  $s/d$  of 3, the piles of CPRF undergoes large moment at the interface between liquefiable and non-liquefiable layer, which recommends that the selection of pile spacing in CPRF should be selected appropriately. The analyses also portray the improvement in PWP ratio near the pile surface when a CPRF system is used in place of a conventional pile group foundation. This effect also confirms the local densification of soil near the piles and the beneficial usage of raft as it helps improving the confining stress in the soil. Effect of pile length is also investigated here. Four  $l/d$  ratios of 14, 16, 18 and 20 are considered for the analyses. From the outcomes, it is concluded that an increase in the shear resistance of piles in CPRF of 40% to 70% can be observed over the pile groups

with the increase in length. It is also noted that for pile groups with shorter pile length which is terminated in the liquefiable zone, after experiencing the maximum shear resistance at the top, the piles encounter drastic reduction in shear resistance along the liquefaction zone. On the contrary, for the piles in CPRF, this decrease in shearing resistance is much lesser and the piles maintain relatively higher resistance all along its length. This response may be caused due to the increased stiffness of piles in CPRF. Moreover, the piles which are founded in competent stratum below the liquefiable zone, demonstrates relatively consistent shear resistance along the length. The bending moment profiles of different piles in CPRF and pile group substantiates that for larger pile lengths, the maximum moment occurs at the juncture of liquefiable soil, whereas the top nodes of piles in CPRF experience much lesser moment than pile group. For shorter pile lengths terminating at the liquefiable zone, the top nodes of both types of piles experience larger moments. Here also, the PWP ratio for CPRF in the mid layer is lower than the same measured for a pile group foundation. These again assert the advantages of using CPRF over pile group in liquefiable area. For investigating the behaviour of these foundation systems more profoundly, analyses are carried out with real seismic loading. Three different earthquake acceleration-time histories, namely 1940 El-Centro, 1989 Loma-Prieta and 2011 Sikkim earthquakes, are chosen for fulfilling this objective. The reason behind choosing these earthquake records is that these seismic data cover a good range of predominant frequencies, PGA and dynamic time, which can be considered to be a good representation of the performance of CPRF and pile group in a dynamic condition. In all the cases, it can be seen that the PWP ratio measured at the middle of the liquefiable zone is less for the case of CPRF than the same for pile group. This phenomena again stipulates the effect of increasing effective stress in the liquefiable layer due to raft in CPRF, which is absent in the pile group. At the top of the liquefiable zone, for both types of foundations, the soil liquefies. Here, the effect of amplification of ground motion in the liquefiable zone is also noteworthy. An increase in the shearing resistance at the top nodes for piles in CPRF of 50% to 80% is observed over the pile group. Although the pile group maintains almost constant shear resistance along its length, the same for CPRF decreases with it. Comparing the bending moments of piles in CPRF and pile group, it can be concluded that for all the cases, the maximum moment is generated at the top of the piles while along the length of the piles, CPRF experiences lesser moment than its pile group counterpart. These findings aid in electing pertinent foundation system to be used in a liquefaction prone areas, where earthquake events are expected.

#### 5. ACKNOWLEDGEMENT

Authors want to acknowledge the financial support received through sponsored research project Grant Number 36(2)/15/04/2016-BRNS/36004-36029 (16BRNS012) from Board of Research in Nuclear Sciences, Department of Atomic Energy, Government of India, for carrying out the research work presented in this paper.

#### 6. REFERENCES

Abdoun, T., Dobry, R., O'Rourke, T. D., and Goh, S. H. (2003) "Pile response to lateral spreads: centrifuge modeling". *Journal of Geotechnical and Geoenvironmental engineering*, 129, Issue 10, 869-878.

Burland, J. B., Broms, B. B., and De Mello, V. F. B., (1977) "Behaviour of foundation and structures", *Proceedings of 9<sup>th</sup> International Conference on Soil Mechanics and Foundation Engineering*, London, 2, pp495-546.

Byrne, P., (1991) "A cyclic shear-volume coupling and pore-pressure model for sand", *Proceedings of 2<sup>nd</sup> International Conference on Recent Advances in Geotechnical Earthquake Engineering and Soil Dynamics*, St. Louis, Missouri, pp47-55.

Chatterjee, K., and Choudhury, D. (2018) "Influence of seismic motions on behavior of piles in liquefied soils". *International*

- Journal for Numerical and Analytical Methods in Geomechanics, 42, Issue 3, pp516-541.
- Chatterjee, K., Choudhury, D. and Poulos, H. G. (2015) "Seismic analysis of laterally loaded pile under influence of vertical loading using finite element method". *Computers and Geotechnics*, 67 pp172-186.
- Chatterjee, K., Choudhury, D., Rao, V. D., and Poulos, H. G. (2019) "Seismic response of single piles in liquefiable soil considering P-delta effect". *Bulletin of Earthquake Engineering*, 17, pp1-27, doi: 10.1007/s10518-019-00588-2.
- Choudhury, D., Phanikanth, V. S., Mhaske, S. Y., Phule, R. R. and Chatterjee, K. (2015). "Seismic liquefaction hazard and site response for design of piles in Mumbai city". *Indian Geotechnical Journal*, 45, Issue 1, pp62-78.
- Dash, S. R., Govindaraju, L., and Bhattacharya, S. (2009) "A case study of damages of the Kandla Port and Customs Office tower supported on a mat-pile foundation in liquefied soils under the 2001 Bhuj earthquake". *Soil Dynamics and Earthquake Engineering*, 29, Issue 2, pp333-346.
- Ghosh, B., and Madabhushi, S. P. G. (2007) "Centrifuge modelling of seismic soil structure interaction effects". *Nuclear Engineering and Design*, 237, Issue 8, pp887-896.
- Horikoshi, K., Matsumoto, T., Hashizume, Y., and Watanabe, T. (2003a) "Performance of piled raft foundations subjected to dynamic loading". *International Journal of Physical Modelling in Geotechnics*, 3, Issue 2, 51-62.
- Horikoshi, K., Matsumoto, T., Hashizume, Y., Watanabe, T., and Fukuyama, H. (2003b) "Performance of piled raft foundations subjected to static horizontal loads". *International Journal of Physical Modelling in Geotechnics*, 3, Issue 2, pp37-50.
- Ibrahim, K., Bunce, G., and Murrells, C., (2009) "Foundation design for the Pentominium tower in Dubai, UAE", *Proceedings of the Institution of Civil Engineers-Civil Engineering*, 162, Issue 6, pp25-33.
- ICG (Itasca Consulting Group), Inc. (2009) *FLAC3D: Fast Lagrangian Analysis of Continua Version 4.0*. Itasca Consulting Group, Minneapolis, MN, USA.
- Katzenbach, R., and Choudhury, D. (2013) *ISSMGE combined pile-raft foundation guideline*. International Society for Soil Mechanics and Geotechnical Engineering (ISSMGE) TC212 Design Guideline. Technische Universitat Darmstadt, Darmstadt, Germany, pp1-23.
- Katzenbach, R., Leppla, S., and Choudhury, D. (2016) *Foundation Systems for High-Rise Structures*. CRC Press, Taylor and Francis Group, UK, (ISBN: 978-1-4978-4477-5), pp1-298.
- Kumar, A., and Choudhury, D. (2016) "DSSI analysis of pile foundations for an oil tank in Iraq", *Proceedings of the Institution of Civil Engineers-Geotechnical Engineering*, 169, Issue 2, 129-138.
- Kumar, A., and Choudhury, D. (2017) "Load sharing mechanism of combined pile-raft foundation (CPRF) under seismic loads". *Geotechnical Engineering, Journal of the Southeast Asian Geotechnical Society (SEAGS)*, 48, Issue 3, pp95-101.
- Kumar, A., and Choudhury, D. (2018) "Development of new prediction model for capacity of combined pile-raft foundations". *Computers and Geotechnics*, 97, pp62-68.
- Kumar, A., Choudhury, D., and Katzenbach, R., (2015) "Behaviour of Combined Pile-Raft Foundation (CPRF) under Static and Pseudo-static Conditions using PLAXIS3D", *Proceedings of the 6th International Conference on Earthquake Geotechnical Engineering (6ICEGE)*, New Zealand, pp1-8.
- Kumar, A., Choudhury, D., and Katzenbach, R. (2016) "Effect of earthquake on combined pile-raft foundation". *International Journal of Geomechanics*, 16, Issue 5, pp04016013.
- Kumar, A., Choudhury, D., and Shin, E. C. (2017a) "State-of-the-art practices on sustainable foundation solutions for high-rise structures using combined pile-raft foundation". *Journal of Urban Science*, 6, Issue 2, pp1-14.
- Kumar, A., Patil, M., and Choudhury, D., (2017b) "Soil-structure interaction in a combined pile-raft foundation-a case study", *Proceedings of the Institution of Civil Engineers-Geotechnical Engineering*, 170, Issue 2, pp117-128.
- Matsumoto, T., Fukumura, K., Horikoshi, K., and Oki, A. (2004) "Shaking table tests on model piled rafts in sand considering influence of superstructures". *International Journal of Physical Modelling in Geotechnics*, 4, Issue 3, pp21-38.
- Phanikanth, V. S., Choudhury, D. and Reddy, G. R. (2013) "Behaviour of single pile in liquefied deposits during earthquakes". *International Journal of Geomechanics*, 13, Issue 4, pp454-462.
- Poulos, H. G. (1994) "An approximate numerical analysis of pile-raft interaction". *International Journal for Numerical and Analytical Methods in Geomechanics*, 18, Issue 2, pp73-92.
- Poulos, H. G. (2001) "Piled raft foundations: design and applications". *Géotechnique*, 51, Issue 2, pp95-113.
- Poulos, H. G. (2016) "Tall building foundations: design methods and applications". *Innovative Infrastructure Solutions*, 1, Issue 1, 10.
- Poulos, H. G. (2017) *Tall Building Foundation Design*. CRC Press, Taylor and Francis Group, UK, (ISBN: 978-1-1387-4803-3), pp1-532.
- Poulos, H. G., and Davids, A. J. (2005) "Foundation design for the emirates twin towers, Dubai". *Canadian Geotechnical Journal*, 42, Issue 3, pp716-730.
- Poulos, H. G., Small, J. C., and Chow, H. (2011) "Piled raft foundation for tall buildings". *Geotechnical Engineering, Journal of the Southeast Asian Geotechnical Society (SEAGS)*, 42, Issue 2, pp78-84.
- Reul, O., and Randolph, M. F. (2004) "Design strategies for piled rafts subjected to non uniform vertical loading". *Journal of Geotechnical and Geoenvironmental Engineering*, 130, pp1-13.
- Roy, J., Kumar, A., and Choudhury, D. (2018) "Natural frequencies of piled raft foundation including superstructure effect". *Soil Dynamics and Earthquake Engineering*, 112, pp69-75.
- Russo, G., Abagnara, V., Poulos, H. G., and Small, J. C. (2013) "Re-assessment of foundation settlements for the Burj Khalifa, Dubai". *Acta Geotechnica*, 8, Issue 1, pp3-15.
- Viggiani, C. (2001) "Analysis and design of piled raft foundations". *First Arrigo Croce Lecture, Rivista Italiana Di Geotechnica*, pp47-75.
- Yamashita, K., Hamada, J., Onimaru, S., and Higashino, M. (2012) "Seismic behavior of piled raft with ground improvement supporting a base-isolated building on soft ground in Tokyo". *Soils and Foundations*, 52, Issue 5, pp1000-1015.